

## FINITE ELEMENT ANALYSIS OF THE CONTACT BETWEEN TOOL AND WORKPIECE AT CERAMIC MATERIALS INTERNAL GRINDING

Daniel POPESCU, Dumitru BOLCU

**Abstract:** Grinding is a processing procedure with small or micro chips. In order to develop in proper conditions, it is necessary a strong correlation between the mechanical characteristics (strength, bending resistance, etc.) of the ceramic product, tool and specific grinding forces. With the FEM analysis the nodal displacements decrease together with the decrease of the transversal contraction coefficient for the same load, while the increase of the elasticity modulus determines also a decrease of the nodal displacements. There are presented the variations of the nodal displacements as function of the longitudinal elasticity modulus  $E$  and of the transversal contraction coefficient  $\nu$  for different types of ceramic materials. The relative deformations for the same load increase with the decrease of the transversal contraction coefficient, while the increase of the elasticity module causes the decrease of the relative deformations.

**Key words:** finite element analysis, internal grinding, ceramic materials.

### 1. INTRODUCTION

Cutting of ceramic materials presents completely different characteristics than those specific to metal processing.

One specific problem is the instability of geometric and technological processing parameters, which determines appearance of defects in the ceramic products, especially in the edge area or at transition between transversal sections. Production of defect-free ceramic pieces is the key factor of measuring their workability and depends directly on both the chip formation mode, which is dependent on the ceramic material nature, and the procedure and parameters of the processing regime, namely cutting tool geometry, mechanical characteristics of the tool material, lubrication, technical characteristics of the machine tool, etc.

Research has shown that fissures generated by the tangential tensions in the cutting zone are larger than radial fissures generated by the normal tensions. Fissure configuration examination indicates that radial fissures have an elliptic shape, while longitudinal fissures have an arrow shape. Both the dimensions and the configuration of the fissures depend mostly on the granularity of the diamond or cubic boron nitride on the cutting tool.

The main difference between internal and external cylindrical grinding consists in the fact that at the same cutting depth  $t$ , the contact is between the active surface of the diamond tool and the concave piece surface, while in the second case the contact is between two convex surfaces. Also, because of the specific grinding scheme, static and dynamic rigidities are reduced at internal cylindrical grinding with respect to external grinding. This influences negatively both the dimensional and geometric precision and the quality of the finished surface, as well as the stability of the grinding process (cutting force, diamond tool endurance, etc.).

### 2. ESTABLISHMENT OF THE FINITE ELEMENT MODEL OF THE CONTACT BETWEEN TOOL AND PIECE IN AXIAL AND TRANSVERSAL DIRECTION

It is considered the static case in which the piece is mounted on the external surface and is in contact with the tool which actions upon the piece with normal force  $F_n$  distributed along  $L_0$  (Fig. 1).

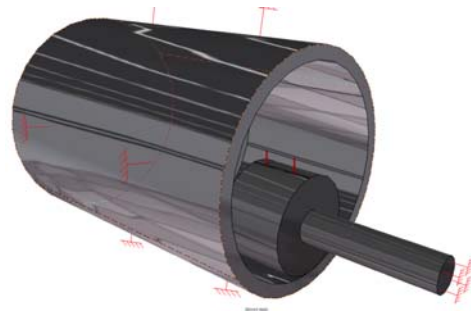


Fig. 1. Static conditions for piece.

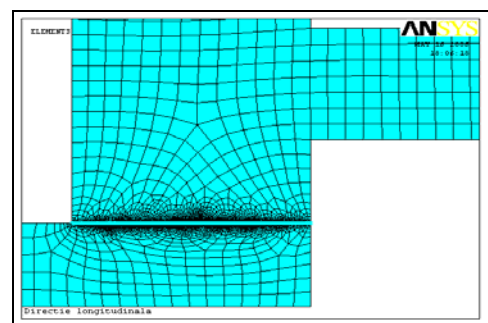


Fig. 2. Definition of contact elements.

It is employed a fine network of 1-mm "Plane82" elements. In the contact area, the network is even finer, while between the two components of the system are

placed special contact elements “Targe169” and “Conta175” (Fig. 2).

In this phase the forces are applied and the model is subjected to constraints. The forces and constraints are applied to the geometry (not in nodes) for facile reuse of the model in case of value, direction or application point changes of the force.

Next are defined the mechanical properties of the workpiece material and abrasive tool respectively. The piece is considered to be manufactured from silicon nitride with longitudinal elasticity modulus  $E = 295$  GPa and transversal contraction coefficient  $\nu = 0.29$ .

Analysis is performed under the assumption that the material linearly-elastic and isotropic. The analysis is non-linear due to the contact between tool and piece.

The distribution of equivalent tensions (von Mises) in case of a distributed force of 10 N/mm along the negative  $Y$  axis is given in Fig. 3 the maximum equivalent tension is 42.211 N/mm<sup>2</sup>.

The distribution and values of the displacements are presented in Fig. 4.

The maximum value of node displacement is  $0.199 \times 10^{-3}$  mm and is situated in the upper left corner of the tool; the minimum values are placed in the mounts.

Next the piece will be considered to be manufactured of Al<sub>2</sub>O<sub>3</sub> (AYCO) with longitudinal elasticity modulus  $E = 360$  GPa and transversal contraction coefficient  $\nu = 0.23$ .

Distribution of equivalent tensions and the nodal displacements for Al<sub>2</sub>O<sub>3</sub> (AYCO) are presented in Fig. 5 and 6.

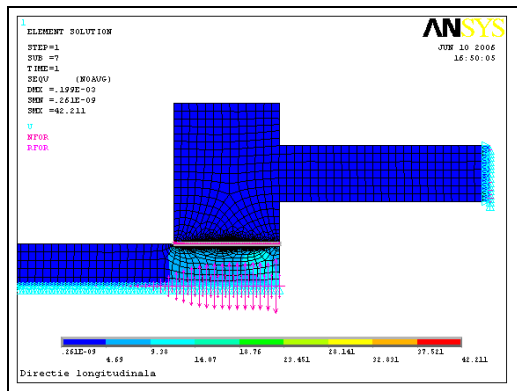


Fig. 3. Distribution of equivalent tensions along  $Y$  axis.

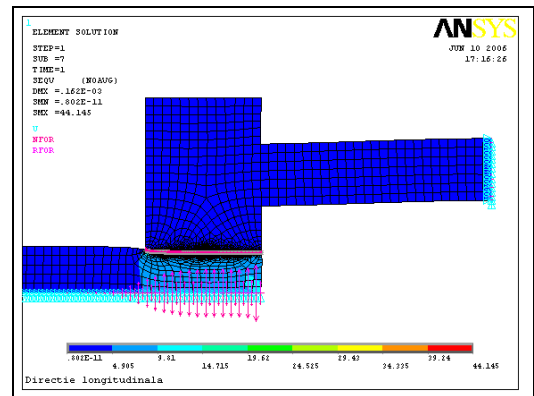


Fig. 5. Distribution of equivalent tensions for Al<sub>2</sub>O<sub>3</sub>.

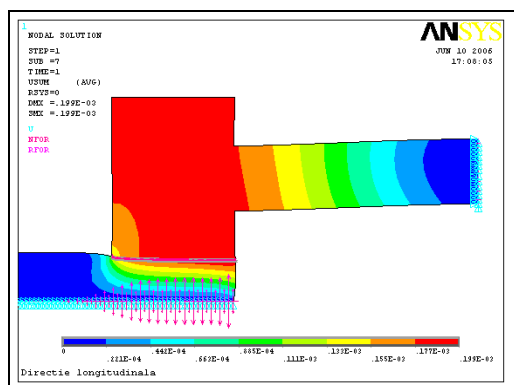


Fig. 4. Displacements distribution and values.

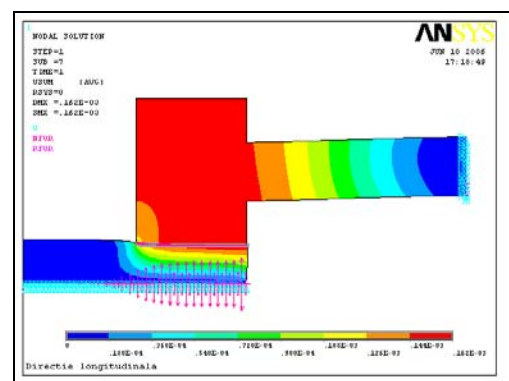


Fig. 6. Nodal displacements (Al<sub>2</sub>O<sub>3</sub> - AYCO).

The maximum displacement for Al<sub>2</sub>O<sub>3</sub> (AYCO) is  $0.162 \times 10^{-3}$  mm.

It is considered a piece manufactured from Al<sub>2</sub>O<sub>3</sub> (LUCALOX) with longitudinal elasticity modulus  $E = 410$  GPa and transversal contraction coefficient  $\nu = 0.23$ . The distribution of tensions is the same as in case of the other materials, and its maximum value is 49.771 N/mm<sup>2</sup>. The maximum displacement in this case is  $0.144 \times 10^{-3}$  mm (Fig. 7).

It is considered a piece manufactured from boron carbide with longitudinal elasticity modulus  $E = 450$  GPa and transversal contraction coefficient  $\nu = 0.2$ . The maximum displacement at the same load is  $0.132 \times 10^{-3}$  mm (Fig. 8).

In case of transversal direction, the discrete plane structure is presented in Fig. 9, in which no element exceeds the shape limits of the tool and workpiece.

It should be noted that the nodes in the inferior part of the tool where the concentrated force will be applied are coupled in  $UY$  (vertical) nodal direction in order to avoid a singularity in the force application point.

In case of transversal direction, the discrete plane structure is presented in Fig. 10, in which no element exceeds the shape limits of the tool and workpiece.

It should be noted that the nodes in the inferior part of the tool where the concentrated force will be applied are coupled in  $UY$  (vertical) nodal direction in order to avoid a singularity in the force application point.

In this phase the model is constraint and the load is applied, defining the type of analysis ant the control elements.

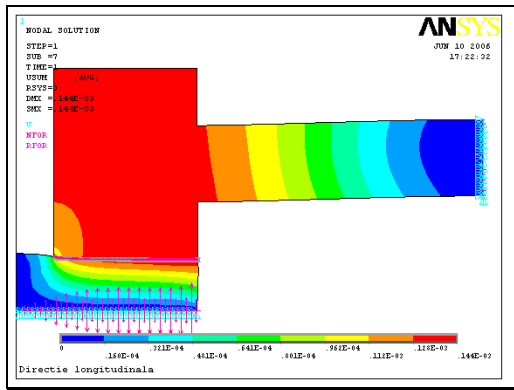


Fig. 7. Nodal displacements ( $\text{Al}_2\text{O}_3$  - LUCALOX).

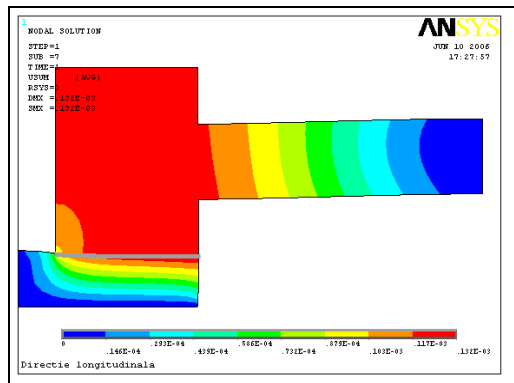


Fig. 8. Nodal displacements (boron carbide).

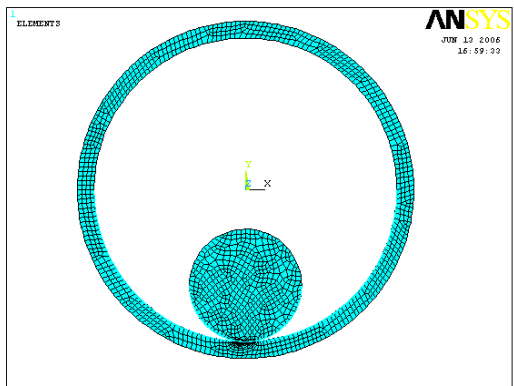


Fig. 9. Transversal plane structure discretization.

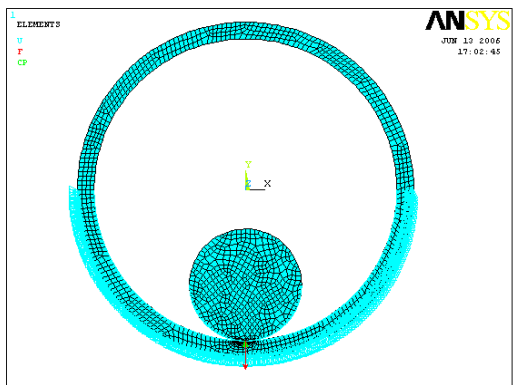


Fig. 10. Definition of the constraint model and application of the distributed force.

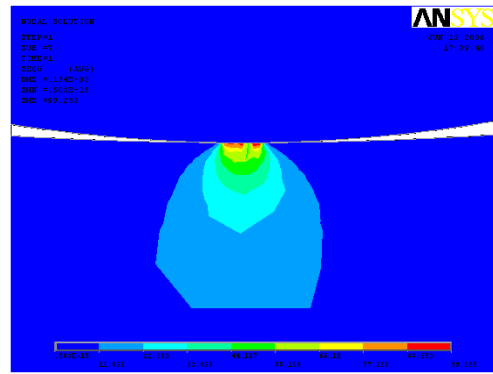


Fig. 11. Maximum equivalent tension distribution.

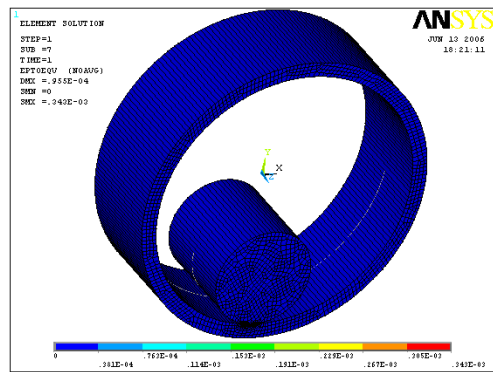


Fig. 12. Equivalent 3D model.

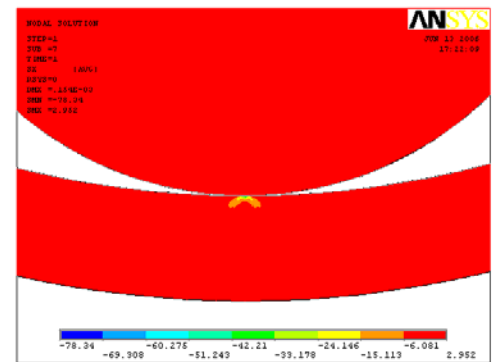


Fig. 13. Tension component along X axis.

The analysis type is static, in which large deformations are allowed, and the minimum and maximum numbers of sub-steps that lead to convergence are 1 and 1000, respectively. The value of the applied force is 300 N.

In the first phase, the piece is considered to be manufactured from silicon nitride with transversal contraction coefficient  $\nu = 0.29$  and longitudinal elasticity modulus  $E = 295$  Gpa.

The maximum equivalent tension (von Mises) is  $99.285 \text{ N/mm}^2$  and its distribution is presented in Fig. 11.

The equivalent 3D model on which analysis is performed is the one from Fig. 12. Its thickness is determined by a real constant taking into account the 20 mm thickness of the plane elements.

Next are presented the tension components along the X and Y coordinate axes (Fig. 13 and 14).

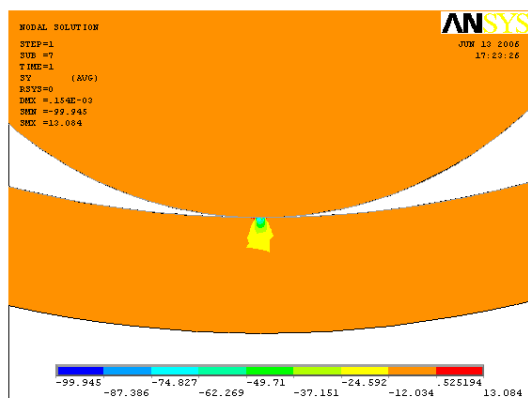


Fig. 14. Tension component along Y axis.

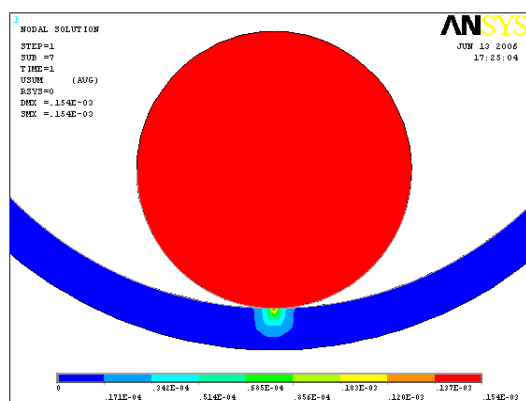


Fig. 14. Nodal displacements.

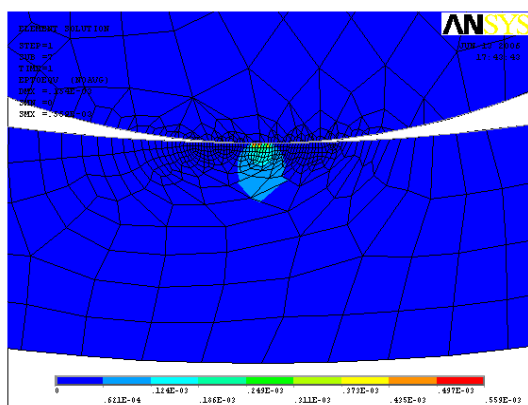


Fig. 15. Relative deformations.

The maximum value of node displacement at 300 N load in case of silicon nitride is  $0.154 \times 10^{-3}$  mm, and the maximum value of relative deformations  $\epsilon$  is  $0.559 \times 10^{-3}$  (Fig. 15).

It can be observed that the largest displacements of the tool are due to the fact that its freedom degrees are constraint only by the contact with the workpiece.

It is considered a piece manufactured of  $\text{Al}_2\text{O}_3$  (AYCO) with longitudinal elasticity modulus  $E = 360$  GPa and transversal contraction coefficient  $\nu = 0.23$ . In what follows only the relative deformations of workpieces from different ceramic materials will be studied.

The maximum deformation value in this case is  $0.458 \times 10^{-3}$  mm.

It is considered a piece manufactured from  $\text{Al}_2\text{O}_3$  (LUCALOX) with longitudinal elasticity modulus  $E = 410$  GPa and transversal contraction coefficient  $\nu = 0.23$ . The maximum relative deformation in this case is  $0.402 \times 10^{-3}$  mm.

It is considered a piece manufactured from boron carbide with longitudinal elasticity modulus  $E = 450$  GPa and transversal contraction coefficient  $\nu = 0.2$ .

In this case, the relative deformation is  $0.366 \times 10^{-3}$  mm.

It is considered a piece manufactured from silicon carbide SiC with longitudinal elasticity modulus  $E = 480$  GPa and transversal contraction coefficient  $\nu = 0.17$ .

In this case the maximum relative deformation is  $0.343 \times 10^{-3}$  mm.

### 3. CONCLUSIONS

The nodal displacements decrease together with the decrease of the transversal contraction coefficient for the same load, while the increase of the elasticity modulus determines also a decrease of the nodal displacements.

It is considered a piece manufactured from silicon carbide SiC with longitudinal elasticity modulus  $E = 480$  GPa and transversal contraction coefficient  $\nu = 0.17$ . In this case the minimum nodal displacement is  $0.124 \times 10^{-3}$  mm, the smallest of all analyzed cases due to high rigidity and low transversal contraction coefficient of the material.

In conclusion, there are presented the variations of the nodal displacements as function of the longitudinal elasticity modulus  $E$  and of the transversal contraction coefficient  $\nu$  for different types of ceramic materials.

The relative deformations for the same load increase with the decrease of the transversal contraction coefficient, while the increase of the elasticity module causes the decrease of the relative deformations.

### REFERENCES

- [1] Kitayama, K. (1992). *Study On Mechanism Of Ceramics Grinding*, Annals of the CIRP, Vol. 41/1/1992.
- [2] Touseff, H.K., Inasaki, I. (1992). *Modelling And Simulation Of Grinding Processes*, Annals of the CIRP, Vol. 41/2/1992.
- [3] Zhang, B., Howes, T.D. (1994). *Material-Removal Mechanism in Grinding Ceramics*, Annals of the CIRP, Vol. 43/1/1994.
- [4] Catia P3 V5R15 Software Suite.
- [5] Oden, J.T., Reddy, J.N. (1976). *An Introduction To The Mathematical Theory of Finite Elements*, New York, London.

### Authors:

PhD, Daniel Popescu, Assoc. Prof., University of Craiova, Department of Technology and Materials, E-mail: daniel.popescu1119@yahoo.com  
PhD, Dumitru Bolcu, Assoc. Prof., University of Craiova, Department of Applied Mechanics, E-mail: dbolcu@mecanica.ucv.ro